Title
SOLID STATE PHYSICS



Author
Crowe, Kenneth M.

Publication Date
1973-06-01

Talk presented at 5th International
Conference on High Energy Physics
and Nuclear Structure, Uppsala,
Sweden, June 18-22, 1973



# SOLID STATE PHYSICS

Kenneth M. Crowe

June 1973

Prepared for the U.S. Atomic Energy Commission
under Contract W-7405-ENG-48

# SOLID STATE PHYSICS

Kenneth M. Crowe

Lawrence Berkeley Laboratory
University of California
Berkeley, California 94720

## ABSTRACT

A review of $\mu^+$ precession experiments is presented. The behavior of the spin of the muon as it interacts in different solids and liquids is discussed, as is muonium formation, "fast" depolarization, and slower relaxation solids and solutions with various chemical and magnetic ions. The interpretation of muonium hyperfine spectra in germanium and silicon, as well as the recently observed anomalous $\mu^+$ precession in silicon, are presented. The use of muons to probe internal magnetic fields in ferromagnets is also reported.

Kenneth M. Crowe

Lawrence Berkeley Laboratory
University of California
Berkeley, California 94720

Muons have played many important roles in physics over the years, as illustrated in Fig. 1. By illuminating the weak interactions, electrodynamics, and nuclear structure, the "heavy electron" has served us well. The positive muon now promises to provide a new probe in its role as the nucleus of the hydrogen-like atom, muonium.[1] Chemical reactions of this light isotope of hydrogen have been studied in gases by Hughes _et al._[2] and in liquids by Brewer _et al._[3] by observing the behavior of the muon's magnetic moment via the asymmetric decay. In liquids, muon depolarization is analyzed in terms of the muonium mechanism developed by Ivanter and Smilga[4] and Brewer,[5] allowing extraction of chemical lifetimes of muonium on a precise time scale from the hyperfine period (1/4 nsec) to several muon lifetimes ( $\sim 10^{-5}$ sec).

Local magnetic fields can be measured by extracting the muon precession frequency from the muon's $\beta$-decay time distribution. The simple model of a $\mu^+$ replacing a proton in a diamagnetic compound provides a probe which complements the nuclear magnetic resonance method for studying liquids and solids. This technique has been reported in several papers.[6,7] In this paper I will limit myself mainly to recent work with positive muons in solids, since the other topics are rather well described in the literature.

The experimental technique used in these studies can be summarized as follows: One allows polarized muons to stop in a target suspended in a known magnetic field. For precession measurements one detects the decay positron, and, with a precise clock, records the time interval from the stopping signature until the decay. Precession appears as a modulation in the distribution of these times, as shown in Fig. 2. Several simultaneous precession signals can be described by the distribution

$$N(t) = N_o e^{-t/\tau_\mu} \left[1 + \sum_i P_i(t) \cos(\omega_i t + \phi_i)\right] + BG,$$

where $\tau_\mu$ is the muon lifetime, $\omega_i = \frac{g}{2} \frac{e(H_{local})}{mc}$ is a precession frequency, $P_i(t)$ is the corresponding effective asymmetry (often exhibiting relaxation), $\phi_i$ is the relative phase,and BG is a constant background. By accumulating a large number ( $\sim 10^6$-$10^7$) of decay events and Fourier analyzing the above time distribution, one can measure the amplitudes of muon precession in various local fields in the same target.

If the muon is located in a muonium atom, the energy levels follow the characteristic Breit-Rabi diagram, shown in Fig. 3, as a function of the external magnetic field. Half of the muonium atoms form in the (F = 1, m = +1) state and half in a superposition of (F = 1, m = 0) and (F = 0, m = 0). In weak fields, to a good approximation, for the first half the muon spin precesses about the external field at a frequency determined by the magnetic moment of the electron (103 times faster than the free muon precession), while for the second half the muon spin flips back and forth at the hyperfine frequency $\omega_o = 2\pi\nu_o$. In stronger fields (comparable to the effective hyperfine field, 1588G), the observable frequencies are the differences shown in Fig. 3, $\omega_{ij} = 2\pi\nu_{ij}$.

For muons stopping in quartz, Gurevich et al. showed[8] that there was a beating of $\omega_{12}$ vs. $\omega_{23}$, whose quadratic field dependence could be analyzed to extract $\omega_o$. They found $\omega_o$ (quartz) approximately the same as $\omega_o$(vacuum). On the other hand, in germanium they found $\omega_o(Ge)/\omega_o(vac) = 0.58(4)$.

We have made similar measurements in silicon. Figure 4 shows a comparison between Fourier transform data for quartz and silicon in the same field. The two highest frequencies correspond to $\omega_{12}$ and $\omega_{23}$ of muonium. Their separation is proportional to $1/\omega_o$ and is clearly larger for silicon. Analysis yields $\omega_o(Si)/\omega_o(vac) = 0.444(20)$.

These results have been satisfactorily interpreted by Wang and Kittel in a recent paper.[9] Their model has muonium trapped in an interstitial site which is large enough to contain the orbital electron in the ground state. Roughly speaking, the binding potential is cut off at large radius due to screening by the valance band electrons of the surrounding atoms of silicon. By using other data they can explain the size of the change in the hyperfine frequency as well as the difference between Ge and Si in terms of the increase in the size of the muonium atom caused by the neighboring atoms of the crystal. This model, the deep-donor for muonium in semiconductors, seems to be in accord with observations. Wang and Kittel observe that "it is not possible at present to compare these values with those for atomic hydrogen---since the presence of atomic hydrogen has never actually been detected---." Further, "we know more about muonium in Ge and Si than about H or $H_2$ in just these crystals on which rests most of modern solid state electronics technology."

In Fig. 4 one can see that there are other Fourier components in addition to the two muonium lines. One expects that the free muon will appear in this figure near zero. However, there are two "stronger" lines at intermediate frequencies, which we have labelled "anomalous precession." We have varied the field in an attempt to follow these lines; Fig. 5 shows the data we have accumulated to date. The two sets of points are associated with different crystal orientations, i.e.[111] and [100], along the field axis. The data are taken with the sample at liquid $N_2$ temperature, for mildly p-type silicon. Both anomalous precession and muonium precession have a lifetime on the order of 300 nsec. Neither of these signals has been detected in n-type Si at $77^oK$ or in any silicon sample at room temperature.

The anomalous frequencies are much higher than the free muon precession frequencies in weak magnetic fields. The muon must therefore be coupled to a particle or system with a larger magnetic moment than its own, as in muonium where it is coupled to an electron by the contact interaction. The field dependence of the data can in fact be fitted to frequencies $\nu_{12}$ and $\nu_{34}$ of a modified Breit-Rabi formula (see Fig. 3), if the different crystal orientations are treated as separate cases. However, it is necessary to allow both the hyperfine coupling strength and the g-factor of the electron to vary in order to obtain a fit. For the case of the [111] crystal axis parallel to the field, the best value for $\nu_o/\nu_o$(vac) is 0.0198(2); for [100] parallel to the field, the best value is $\nu_o/\nu_o$(vac) = 0.0205(3). In both cases, the best value for $g_e$ is 13±3. Clearly, the spin g-factor of an electron cannot be much different from 2, nor can a pure contact interaction be anisotropic; this modified Breit-Rabi description is meant only as a phenomenological characterization of the data.

These results can be interpreted in terms of several physical models. Perhaps the simplest is shallow-donor muonium. Here the electron wave function is spread over many lattice sites, whereas the entire deep-donor muonium atom fits into one interstitial site. An s-state cannot produce the observed behavior, due to the relatively invariable spin g-factor of the electron. However, in the 2p state the orbital g-factor can be large and anisotropic: the electron wave function for a shallow donor must be a superposition of conduction band states, which may have small, anisotropic effective masses. A possible objection to this model is the requirement of a minimum lifetime of $\sim$ 300 nsec for the 2p excited state. Hindrance of the normally fast radiative E1 transition 2p $\rightarrow$ 1s can be explained by the small overlap between electron wave functions in the shallow-donor 2p state and the deep-donor 1s state.

A second physical model is suggested by the large variety of ESR centers which have been observed in radiation-damaged silicon.[10] The muon may create a paramagnetic lattice defect (e.g., a broken bond) at the end of its range, combining with it to form a muon-defect bound state. Such a center can also be described by a modified Breit-Rabi hamiltonian.

The possibility that the anomalous precession is due to formation of a bound state of a muon with an impurity atom is considered remote.

However, in stopping, the muon must generate a high density of free electrons and holes, with which it may subsequently combine. If we regard the $\mu^+$ as a positive impurity ion in an interstitial position, observations of impurity-exciton bound states in silicon provide a precedent for two models involving excitons. The first model is the neutral muonium-exciton molecule ($\mu^+ e^- e^- h^+$), in which the two electrons are assumed to have paired spins, in analogy with ground-state $H_2$. The $\mu^+$ is thus coupled to the hole by a dipole-dipole interaction. Orientational effects are predicted by this model if the molecule is "pinned" by being wedged into an oblong interstitial site in the unit cell. A second model of this type is the ionized muonium-exciton molecule ($\mu^+ e^- h^+$), in which all three particles are coupled via contact interactions. These models draw support from the fact that measured free exciton lifetimes in silicon at $80^\circ$K are about 400 nsec.[11]

None of the above physical models for anomalous muon precession can be eliminated on the basis of existing data; however, we feel that shallow-donor 2p muonium is the most probable explanation.

Let me turn now to the studies by Kossler et al. using muons to probe ferromagnetic materials.[12] The reference contains an abundance of data; I will only discuss the experimental aspects which we have pursued.

The experiment is similar to those mentioned previously. One places a nickel sample in a magnetic field ($B_{ext}$), and looks for muon spin precession. Surprisingly, there is a large signal, from which the local field at the muon ($B_\mu$) can be extracted.

For external fields too weak to saturate the sample, $B_\mu$ is independent of $B_{ext}$. This is due to the high permeability of the nickel: domain walls can easily move to screen out the external field. Above saturation, no further wall motion can occur, and $B_\mu$ rises linearly with $B_{ext}$ (see Fig. 6).

$B_\mu$ is strongly temperature dependent, as shown in Fig. 7. The behavior is similar to that of the saturation magnetization ($M_s$): i.e., a Brillouin function. As one raises the temperature through the Curie point, $B_\mu$ abruptly becomes equal to the external field; and the muons precess in a paramagnetic environment.

Another interesting effect is the depolarization of the muons, reflected in the decay of the precession signal. This depolarization may be due either to dephasing in an inhomogeneous local field or to relaxation phenomena. Short depolarization times were observed for muons in polycrystalline samples, including ours, which was ellipsoidal in shape in order to produce a uniform macroscopic internal field. The temperature dependence of the depolarization time is shown in Fig. 8. These results can be explained in terms of local field inhomogeneities produced by the random orientation of individual crystallites: the temperature dependence arises from the temperature-dependent anisotropy field, which strives to orient the local magnetization along the easy axis. The sharp drop in the depolarization time observed as the Curie temperature is approached is probably due to imperfect thermal regulation in a region where $B_\mu$ is changing very rapidly with temperature (see Fig. 7).

The depolarization becomes very pronounced at room temperature, where precession is observed in an annealed sample only near saturation, and is barely detectable in an unannealed sample. In a single crystal sample, however, long-lived precession is observed even at liquid $N_2$ temperature.

There are a number of interesting questions which present themselves: What is the coupling between $B_\mu$ and $M_s$ which causes them to have basically the same temperature dependence? Are there deviations from this simple proportionality? Where does the muon sit? Is it hopping from one interstitial site to another? What is the structure of its electron cloud? Since the conduction electrons are polarized negatively in the interstitial region, why does the muon definitely precess in the positive sense?

Another line of questions has to do with the depolarization observations. The local field inhomogeneity can be studied,and perhaps other depolarization mechanisms can be identified.

Finally, are there other frequencies which represent alternate sites or states for the muon?

The study of these questions will doubtless point the way for investigations of other classes of magnetic materials, metals,and alloys.

In summary, the positive muon is alive and well, and living in solids long enough to perform many impressive feats. Following its spin leads to a rapidly expanding vista of applications in solid state physics.

ACKNOWLEDGEMENT

I wish to express my appreciation to J. H. Brewer, F. N. Gygax, R. R. Johnson, B. D. Patterson, D. G. Fleming, and A. Schenck for their participation and assistance in the experimental work and their help in preparing this report.

Work done under the auspices of the U.S. Atomic Energy Commission.

REFERENCES

1. V. W. Hughes, Ann. Rev. Nucl. Sci. 16, 445 (1966).

2. R. M. Mobley, J. M. Bailey, W. E. Cleland, V. W. Hughes and J. E. Rothberg, J. Chem. Phys. 44, 4354 (1966);
R. M. Mobley, J. J. Amato. V. W. Hughes, J. E. Rothberg and P. A. Thompson, J. Chem. Phys. 47, 3074 (1967).

3. J. H. Brewer, K. M. Crowe, R. F. Johnson, A. Schenck and R. W. Williams, Phys. Rev. Lett. 27, 297 (1971).

4. I. G. Ivanter and V. P. Smilga, Soviet Phys. JETP 27, 301 (1968);
I. G. Ivanter and V. P. Smilga, Soviet Phys. JETP 28, 796 (1969);
I. G. Ivanter, Soviet Phys. JETP 29, 761 (1969);
I. G. Ivanter and V. P. Smilga, Soviet Phys. JETP 33, 1070 (1971);
I. G. Ivanter and V. P. Smilga, Soviet Phys. JETP 34, 1167 (1972).

5. J. H. Brewer, F. N. Gygax and D. G. Fleming, (submitted to Phys. Rev. A.)

6. A. Schenck, Physics Letters, Vol. 32A, 1 (1970) , 19.

6A. A. Schenck, D. L. Williams, J. H. Brewer, K. M. Crowe and R. F. Johnson, Chem. Phys. Lett. 12, 544 (1972).

7. A. Schenck and K. M. Crowe, Phys. Rev. Lett. 26, 57 (1971).

8. I. I. Gurevich, I. G. Ivanter, E. A. Meleshko, B. A. Nikol'skii, V. S. Roganov, V. I. Selivanov, V. P. Smilga, B. V. Sokolov and V. D. Shestakov, Soviet Phys. JETP 33, 253 (1971).

9. J. Shy-Yih Wang and C. Kittel, Phys. Rev. B 7, 713 (1973).

10. G. Lancaster, ESR in Semiconductors (Plenum Press, New York 1967).

11. V. S. Vavilov, É. L. Nolle, Soviet Phys. Semicond. 2, 616 (1968).

12. M. L. G. Foy, N. Heiman, W. J. Kossler and C. E. Stronach, Phys. Rev. Lett. 30, 1064 (1973).

## FIGURE CAPTIONS

FIG. 1. Various experiments in progress which utilize the muon as a probe of matter.

FIG. 2. A typical experimental histogram. Carbon tetrachloride at 100 G. The data are binned into 10-nsec bins for clarity; for fitting, 0.5-nsec bins were used. The mean muon lifetime $\tau_\mu = 2.20$ sec is indicated.

FIG. 3. Energy eigenstates of $\ell = 0$ muonium in an external magnetic field, as functions of the dimensionless "specific field" $X = 2\mu_e B/h\nu_o$. The four allowed transitions are indicated. The relation $\nu_{12} + \nu_{34} = \nu_o$ holds for all fields, where $\nu_{12}$ is understood to be negative for $X > X^* \cong (m_\mu - m_e)/2m_e$, where the top two levels cross.

FIG. 4. Frequency spectra of muons in fused quartz at room temperature and in p-type silicon at 77°K. In both cases the applied field is 100 gauss. The vertical axis is the square of the Fourier amplitude, in arbitrary but consistent units. In the lower graph the vertical scale is expanded by a factor of 10 to the right of the dashed line. The prominent peaks (from left to right) are: the free muon precession signal at 1.36 MHz; a characteristic background signal at 19.2 MHz, due to rf structure in the cyclotron beam; the two anomalous frequencies at 43.6 ± 2.9 MHz (silicon only); and the two 1s muonium peaks centered about 139 MHz. The wider splitting of the two 1s muonium lines in silicon is due to the weaker hyperfine coupling. These spectra were produced by Fourier analyzing the first 750 nsec of the experimental histograms.

For comparison, the muon asymmetries obtained by maximum likelihood fits to the first 5 μsec of data were 3.81 ± 0.35 % for quartz and 5.05 ± 0.63 % for p-type Si at 77°K.

FIG. 5. Dependence of anomalous frequencies in silicon upon field strength and crystal orientation. Round points and solid lines are data and best fit for (111) crystal axis along the field; triangular points and dashed lines are data and best fit for (100) axis along the field. Free muon, 1s muonium, and cyclotron background signals are not shown. A number of peaks appear in the spectra in addition to the fitted "proper" anomalous frequencies; these are unexplained. They are indicated by square points (for prominent peaks) and horizontal bars (for weak or questionable peaks). The higher of the "proper" anomalous frequencies is missing at several fields. This is because the spectra showed no statistically significant peaks at those positions.

FIG. 6. The local field $B_\mu$ at the muon site in nickel vs. $B_{ext}$, the external field measured with target out. The points denoted by asterisks are from data on a single crystal with the (111) axis parallel to $B_{ext}$. Other points are from data on an unannealed, polycrystalline ellipsoid (4.5" x 2" x .5"). "Vert" refers to the 4.5" axis parallel to $B_{ext}$, and "Horiz" to the 2" axis parallel to $B_{ext}$.

FIG. 7. The local field at the muon site in nickel ($B_\mu$) vs. temperature, for external fields too small to saturate the samples.

FIG. 8. The depolarization time constant for muons in nickel versus temperature. (Data from Kossler _et al._)

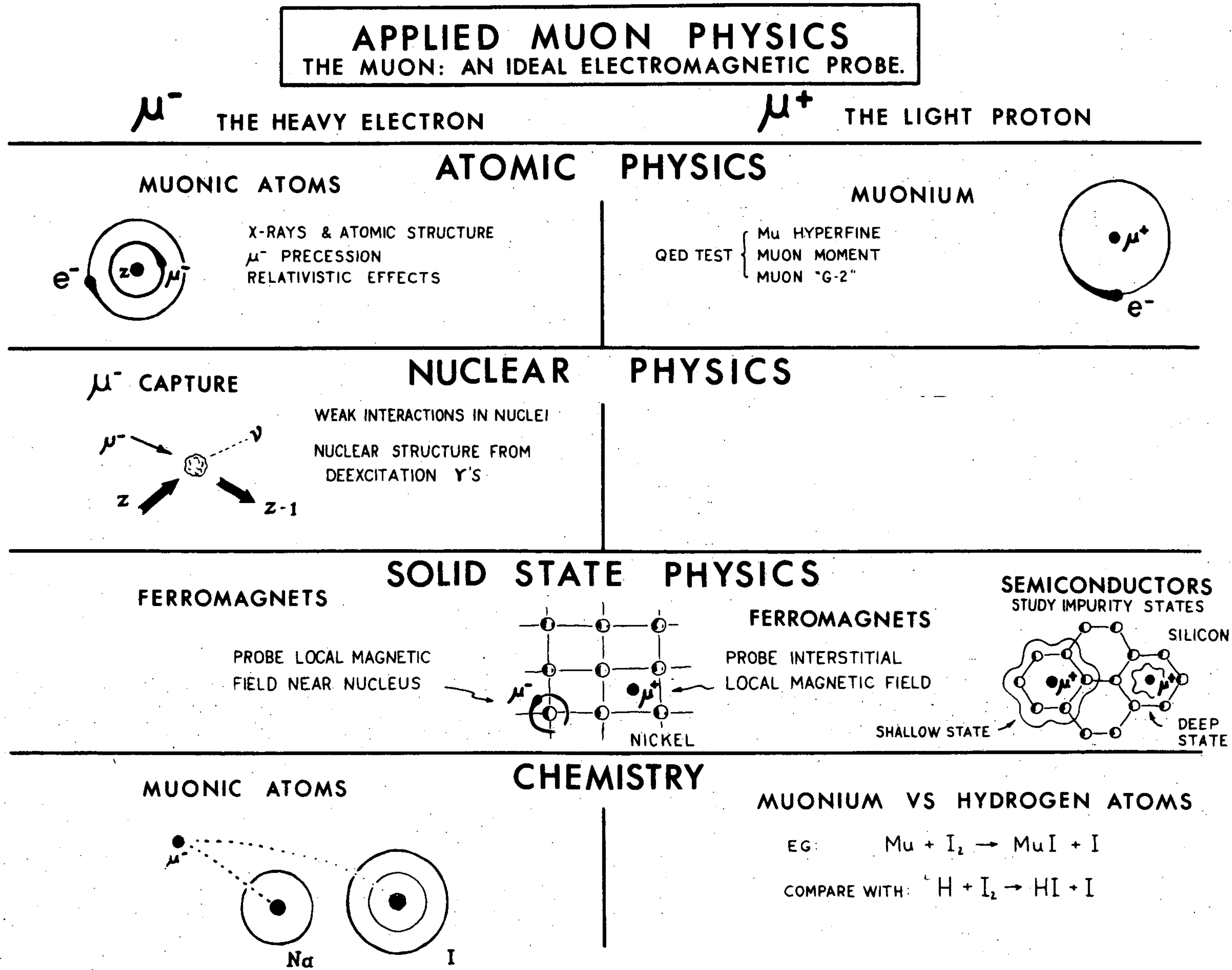

APPLIED MUON PHYSICS
THE MUON: AN IDEAL ELECTROMAGNETIC PROBE.
μ⁻ THE HEAVY ELECTRON
μ⁺ THE LIGHT PROTON
ATOMIC PHYSICS
MUONIC ATOMS
X-RAYS & ATOMIC STRUCTURE
μ⁻ PRECESSION
RELATIVISTIC EFFECTS
e⁻
z
μ⁻
MUONIUM
QED TEST
Mu HYPERFINE
MUON MOMENT
MUON "G-2"
μ⁺
e⁻
NUCLEAR PHYSICS
μ⁻ CAPTURE
μ⁻
ν
z
z-1
WEAK INTERACTIONS IN NUCLEI
NUCLEAR STRUCTURE FROM DEEXCITATION γ'S
SOLID STATE PHYSICS
FERROMAGNETS
PROBE LOCAL MAGNETIC FIELD NEAR NUCLEUS
μ⁻
μ⁺
NICKEL
FERROMAGNETS
PROBE INTERSTITIAL LOCAL MAGNETIC FIELD
SEMICONDUCTORS
STUDY IMPURITY STATES
SILICON
μ⁺
μ⁺
SHALLOW STATE
DEEP STATE
CHEMISTRY
MUONIC ATOMS
μ⁻
Na
I
MUONIUM VS HYDROGEN ATOMS
EG: Mu + I₂ → MuI + I
COMPARE WITH: H + I₂ → HI + I


Fig 1

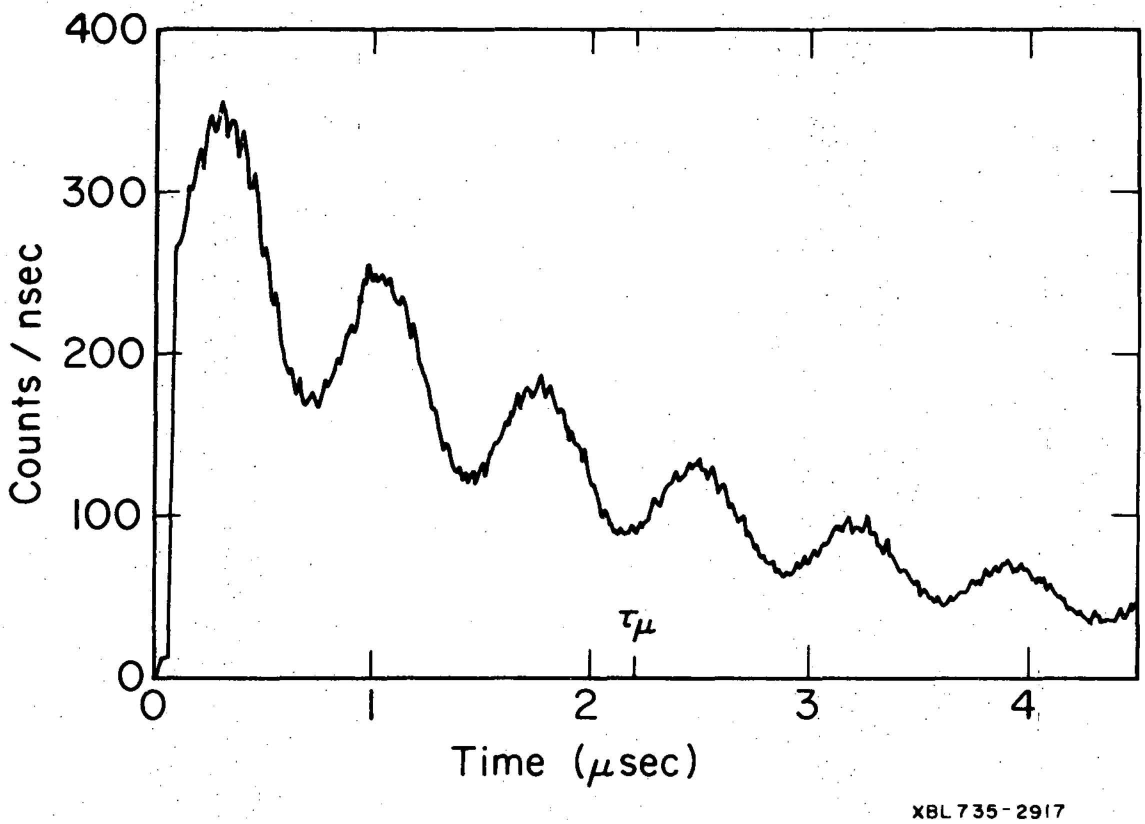


Fig. 2

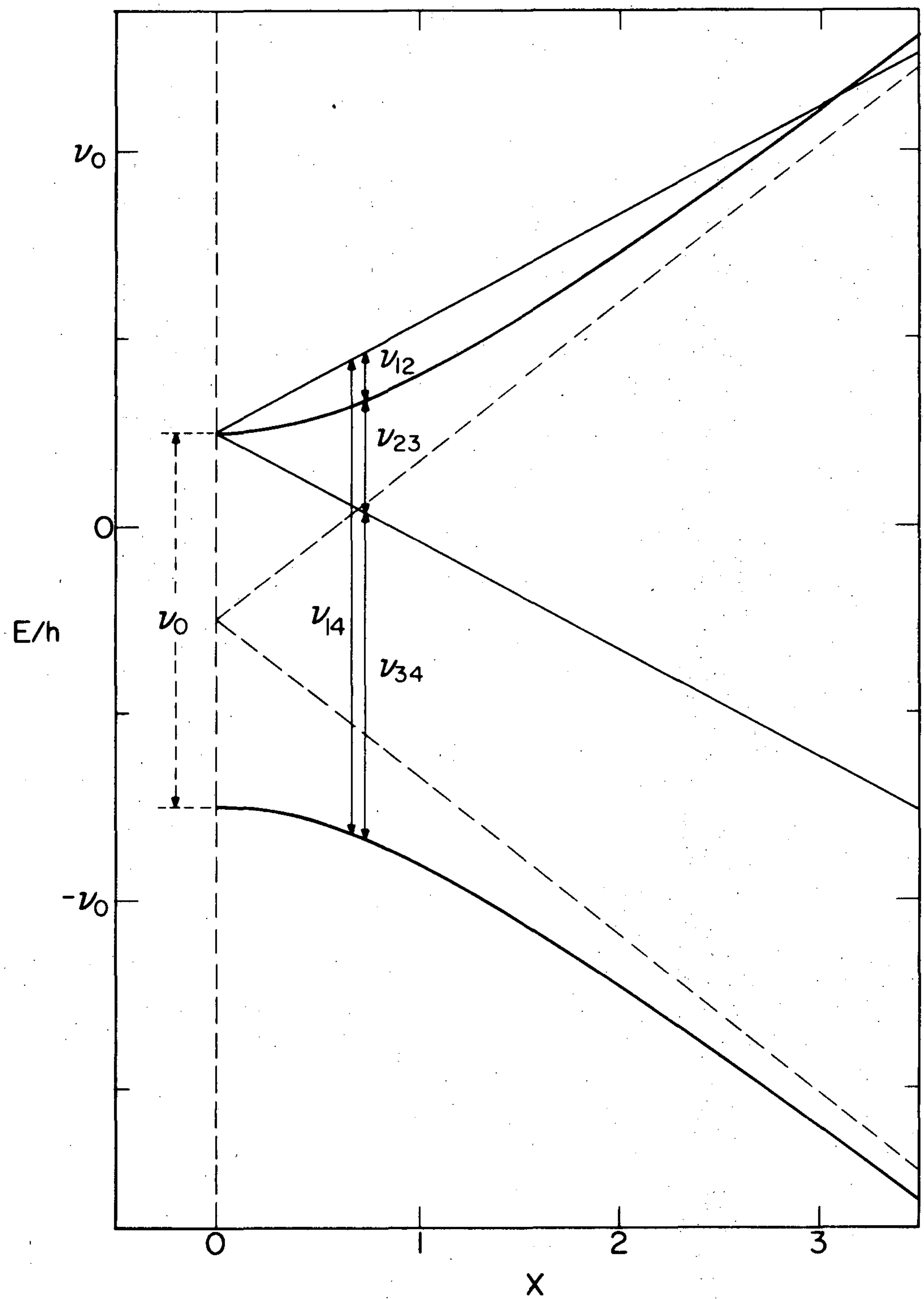


XBL733-2502

Fig. 3

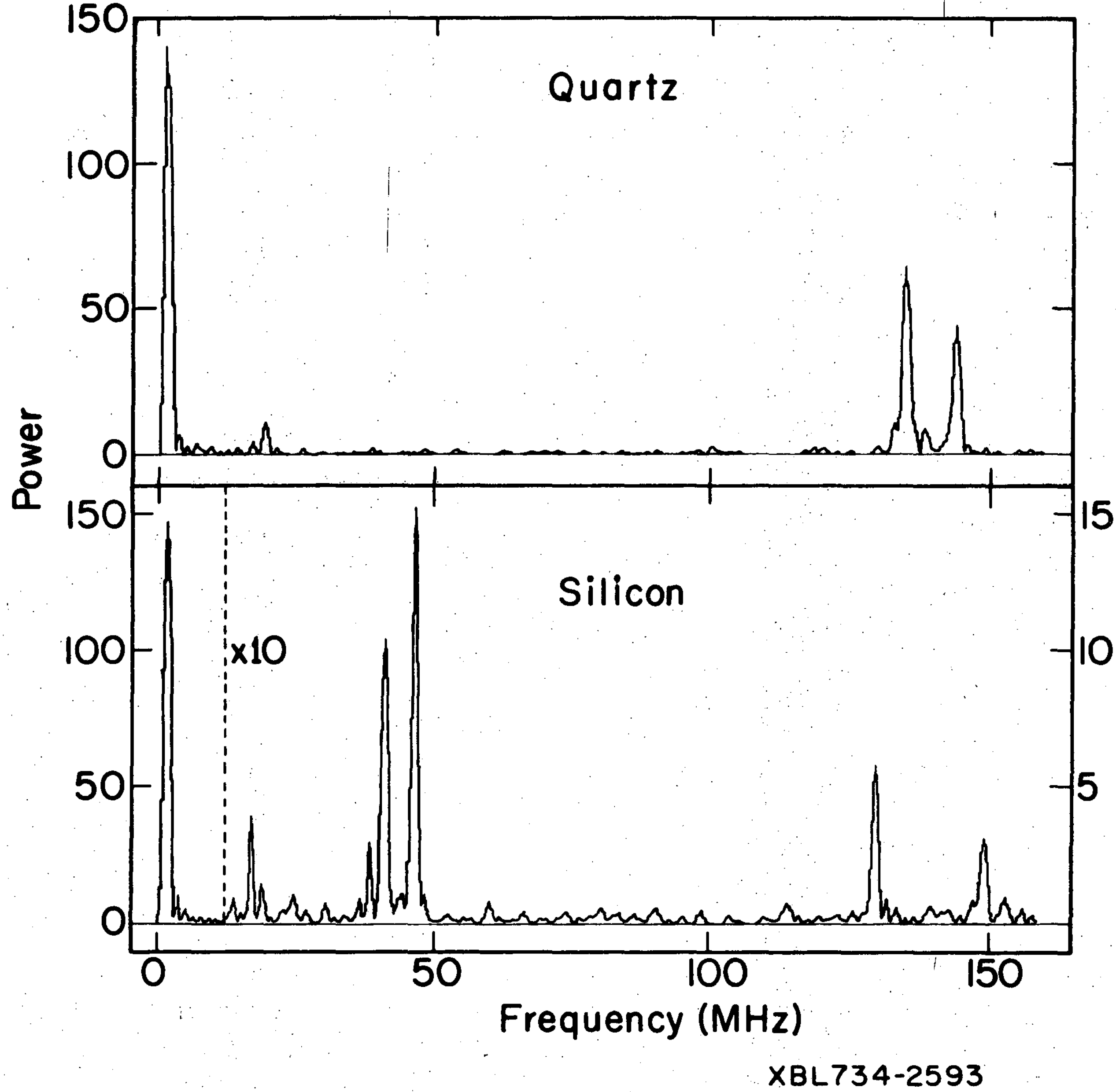
Quartz
Silicon
x10
Power
Frequency (MHz)
0
50
100
150
5
10
15
XBL734-2593

Fig. 4

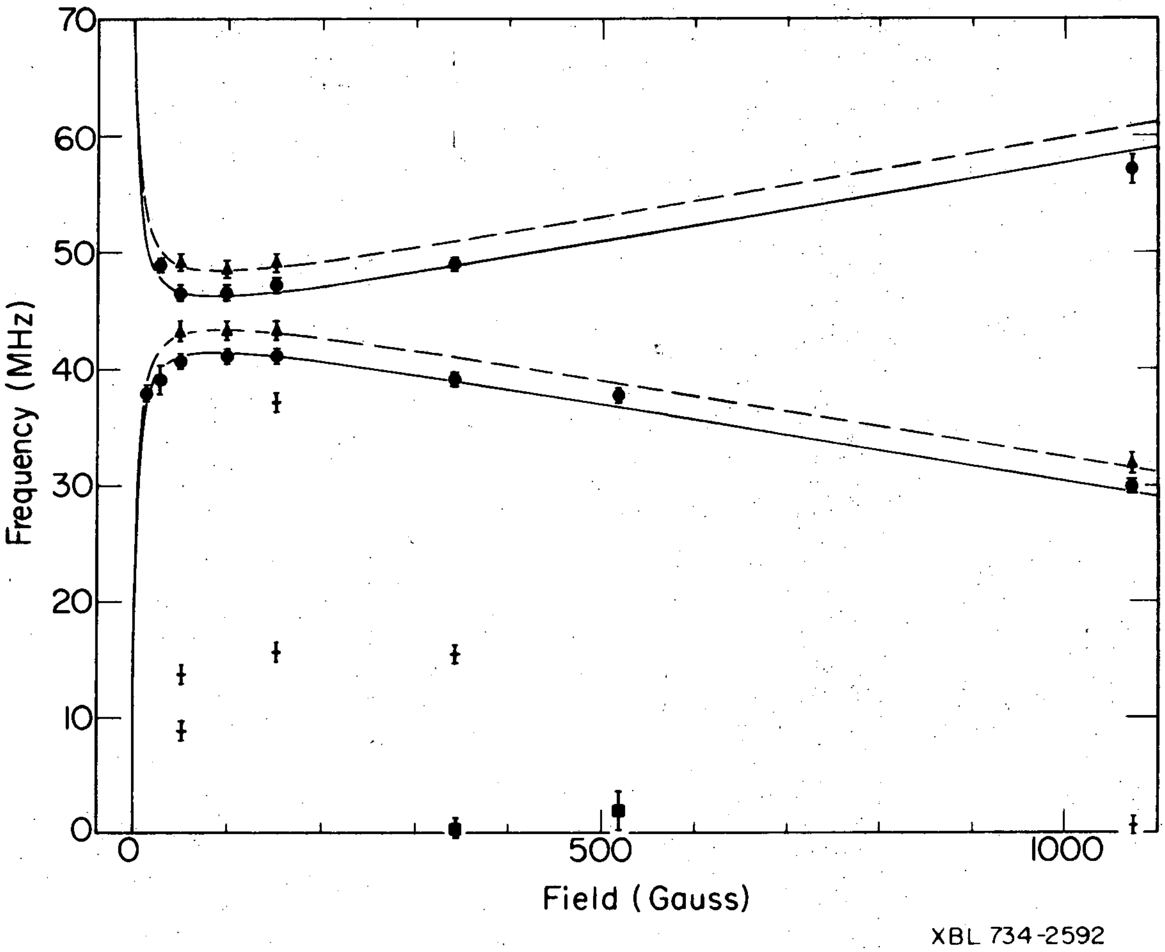
70
60
50
40
30
20
10
0
Frequency (MHz)
0
500
1000
Field (Gauss)
XBL 734-2592

Fig. 5

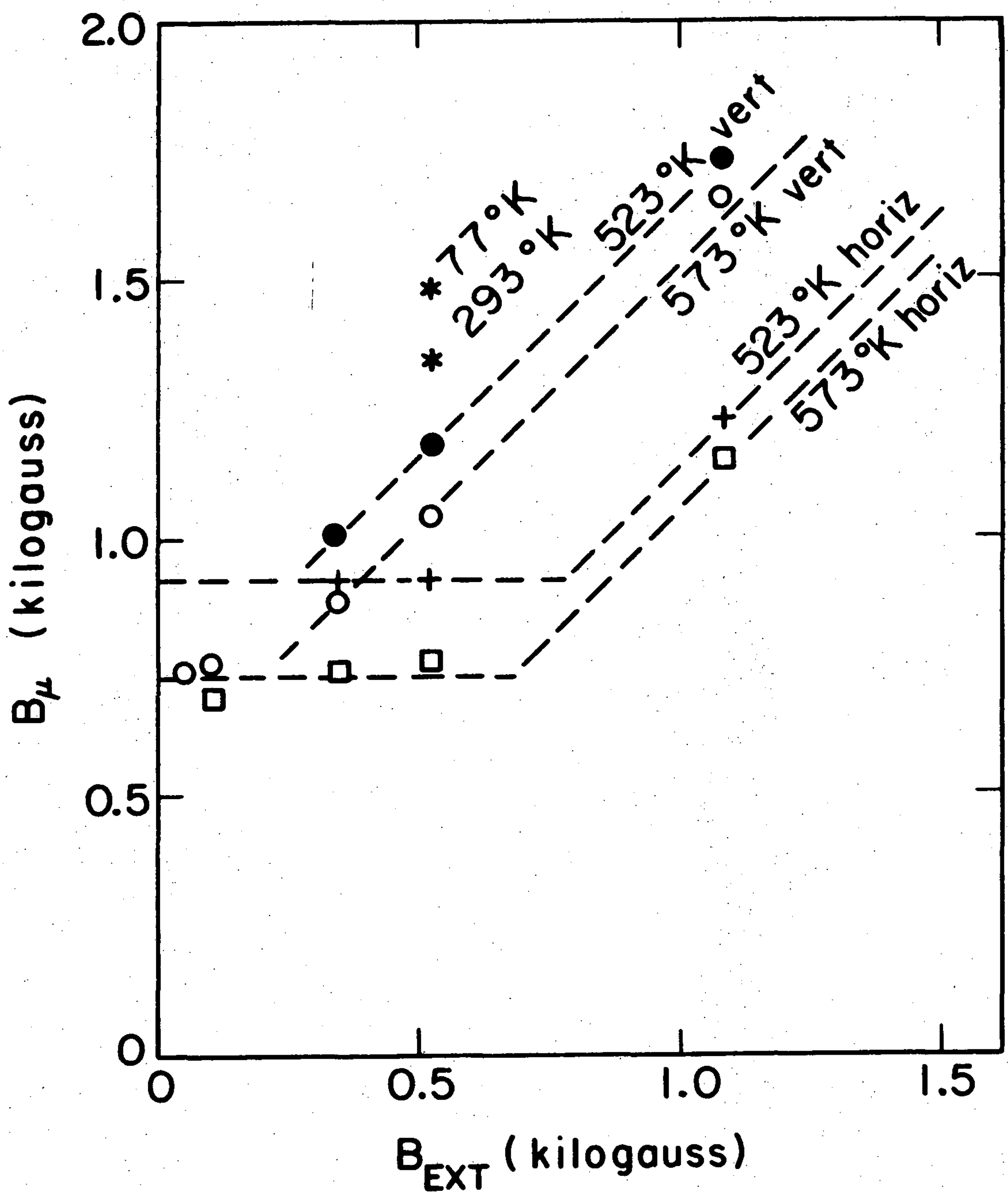


XBL738-3674

Fig. 6

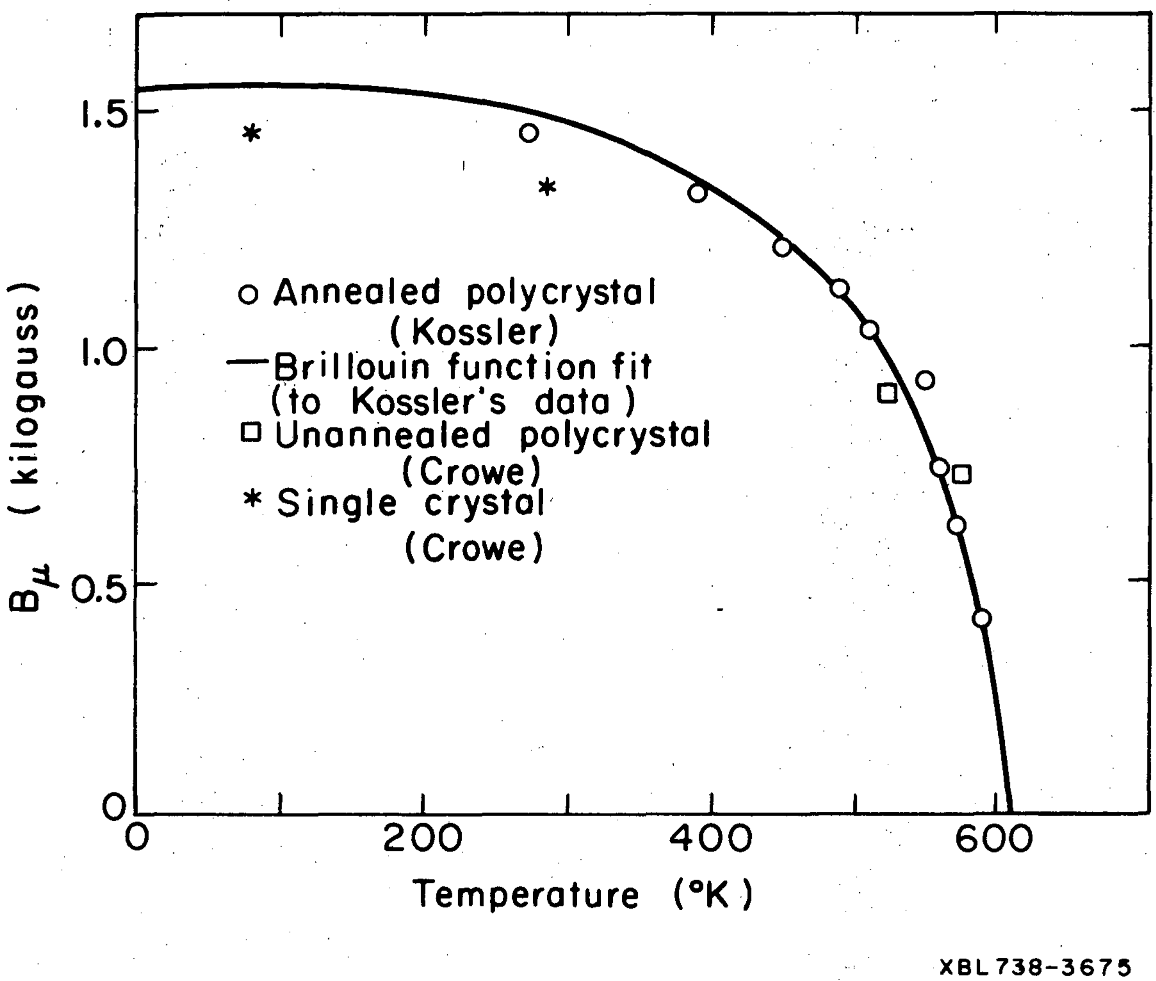

1.5
1.0
0.5
0
$B_\mu$ (kilogauss)
0
200
400
600
Temperature (°K)
o Annealed polycrystal (Kossler)
— Brillouin function fit (to Kossler's data)
□ Unannealed polycrystal (Crowe)
* Single crystal (Crowe)
XBL 738-3675


Fig. 7

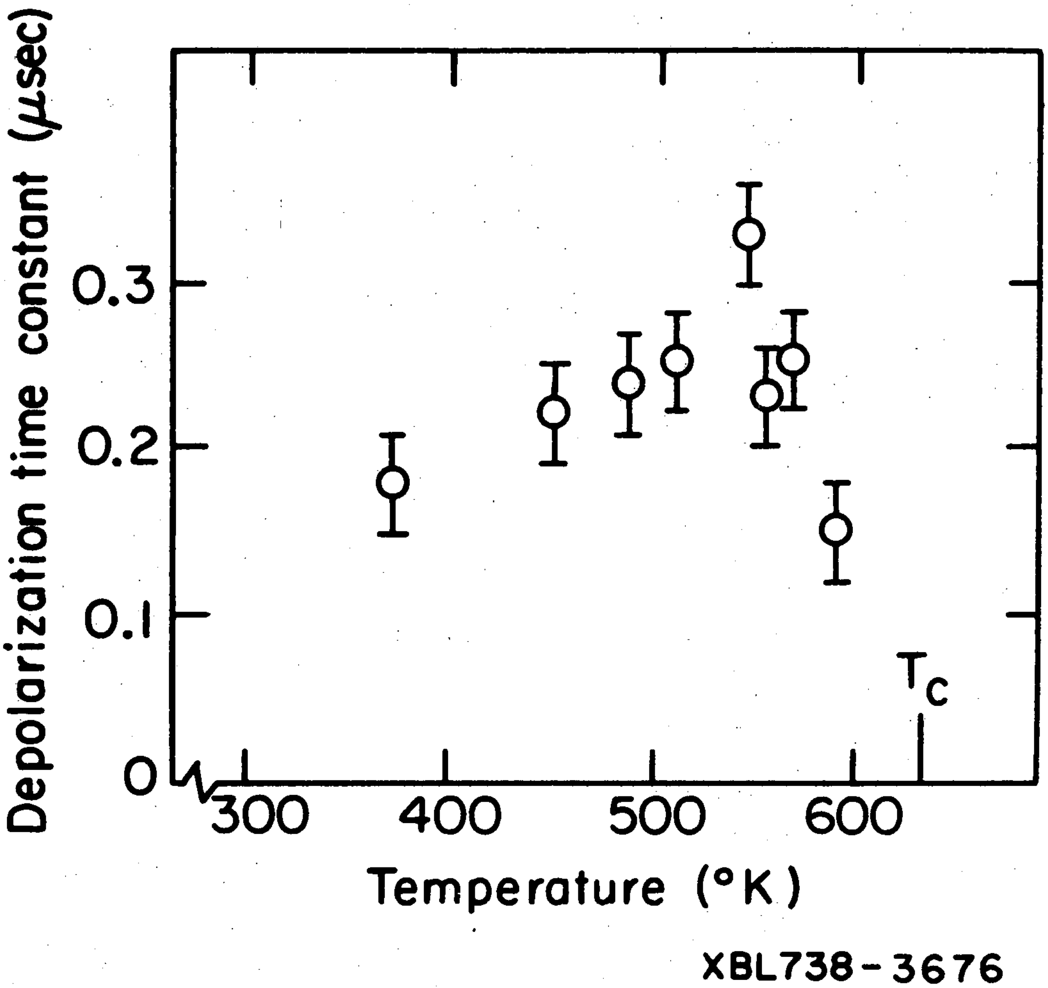
Depolarization time constant (μsec)
0.3
0.2
0.1
0
300
400
500
600
$T_c$
Temperature (°K)
XBL738-3676

Fig. 8

TECHNICAL INFORMATION DIVISION
LAWRENCE BERKELEY LABORATORY
UNIVERSITY OF CALIFORNIA
BERKELEY, CALIFORNIA 94720